

# THE HIGH POWER TEST MODEL OF C-BAND ACCELERATING STRUCTURE FOR COMPACT XFEL AT SINAP\*

W. Fang, Q. Gu, Z. Zhao<sup>#</sup>, SINAP, Shanghai, China  
D. Tong, TUB, Beijing, China

## Abstract

R&D of a C-band (5712 MHz) high gradient traveling-wave accelerating structure is being in progress at Shanghai Institute of Applied Physics (SINAP). Conceptual design of the accelerating structure has been accomplished, and verified by the cold test of the experimental model. Now the first prototype structure is ready for high RF power test and the optimization of a new operating mode is proposed for developing a robust high gradient C-band structure. In this paper, the results of the cold test of the first prototype structure and the optimization details are introduced.

## INTRODUCTION

A compact hard X-ray Free Electron Laser (XFEL) facility is presently being planned, and some analytical and simulation research is ongoing at the Shanghai Institute of Applied Physics [1]. This facility will be located close to the Shanghai Synchrotron Radiation Facility which is a 3rd generation light source in China [2]. It requires a compact linac with a high gradient accelerating structure and high beam quality. At room temperature, linac, the C-band (5712 MHz) accelerating structure, is a compromise and a good option for this compact linac designed to operate at 40 MV/m [3]. In XFEL/SPring-8, the chock-mode-type C-band accelerating structure of 1.8 m is designed to operate at a high accelerating gradient of 35 MV/m (40 MV/m was achieved in 2009). This results in the 8 GeV linac of XFEL/SPring-8 being about 400 m in total length, which is a suitable size for a compact facility compared with similar machines in the United States and Europe [4, 5].

The experimental model has been cold tested and verified on the feasibility [3], and the first high power structure is also ready, both are constant impedance accelerating structures and  $2\pi/3$  mode, and the field distribution is not constant. For the linac to achieve high gradient, the constant gradient field distribution is the optimal choice, and at the same time it needs to be capable of high gradient and high beam quality. To achieve the high constant gradient field and beam quality, the RF breakdown stability and wakefield are two crucial issues in designing the accelerating structure. To optimize this design, many issues are considered and analyzed, such as the pulse compressor, operating mode and disk shape. Here, an optimized scheme with a  $4\pi/5$  mode is proposed.

## COLD TEST OF FIRST PROTOTYPE

After all the brazing step, the C-band accelerating structure is tested by low power RF, and tuned to eliminate the mismatch of couplers and regular cells, at last, the high power model is shown in Fig. 1.



Figure 1: 1<sup>st</sup> prototype C-band accelerating structure.

According to the non-resonant perturbation theory and technique [6, 7], A tuning code based on LABVIEW 8.5 has been written. The amplitude and phase of field distribution on axis are measured and analyzed, and then the mismatch of each cell can be calculated cell by cell independently. According to the mismatch of each cell, the accelerating structure can be tuned cell by cell iteratively under the control of LABVIEW code. After several iterations of tuning, the accelerating structure is matched, and the results are shown in Fig. 2.

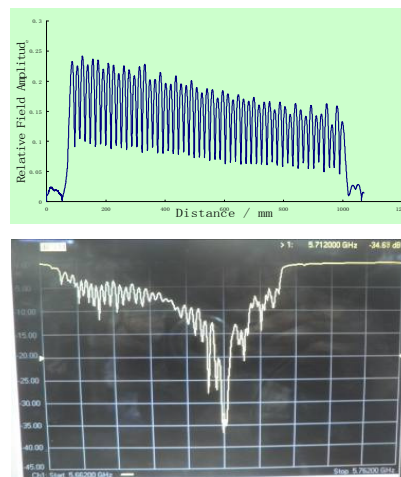


Figure 2: The matching field distribution and S11.

After tuning of all cells and two couplers, the C-band accelerating structure is matched. The field distribution on axis is smooth and the reflection of input port become on

\*Work supported by the Program of the Shanghai Subject Chief Scientist-Natural Science Foundation (08XD1405400)

<sup>#</sup> zhaotz@sinap.ac.cn

axis is smooth and the reflection of input port becomes slight as shown in Fig. 2. The SWR in of input port is below 1.1 corresponding to 2MHz bandwidth, and on the point of center frequency 5712MHz the S11 is about -35dB, and also the same to the field distribution on axis. The results are thus reach the design target, and after the baking, the model can be ready for the high power RF test.

## OPTIMIZATION FOR NEW MODE ACCELERATING STRUCTURE

In order to develop the robust structure for the future application for compact XFEL facility, the optimization of the first prototype of C-band accelerating structure has been analyzed, and a new operating mode is derived after optimizing several issues.

### High Power RF System

For a high constant gradient field, the existing klystron power source of 50 MW cannot meet the power requirement of the field target, and a pulse compressor is required for multiplying the power from klystron.

According to the principles of operation of the first generation pulse compressor (SLED-I) and constant impedance (CI), the suitable combination of SLED-I and CI can give a smart scheme for constant field distribution on axis [8], however this scheme has two shortage: The field amplitude of time is changed during the pulse length, and therefore it is not suitable for a multi-bunch pattern in the future, and the top of the output pulse is not flat, and requires high power at the beginning of the pulse for constant field distribution. Taking a 40 MV/m constant gradient on the axis for example, the peak of the output power of SLED-I should reach 110 MW, and may result in a serious breakdown problem upstream of the CI structure.

The scheme for the CI+SLED-I is a smart solution for constant field distribution on the axis, however it is not stable and extensive enough. In contrast, the constant gradient structure (CG)+SLED-II is an effective and stable solution. The SLED-II is a second generation pulse compressor with a flat-top pulse. When a flat-top power pulse is input into the CG structure, the field of both time and space on the axis is constant, thus the CG+SLED-II is suitable for a multi-bunch pattern and can reduce the rate of RF breakdown.

### Phase Advance, $a/\lambda$ , Phase Stability and Structure Length

To some extent, the operating mode of a traveling-wave accelerating structure is indirectly related to the short - range wakefield (SRW), RF breakdown and phase stability.

In the hard XFEL facility, the peak current of the bunch should reach the order of several thousand Amperes, thus the bunch length is about a millimeter or smaller. For such a short bunch length, the SRW can induce a strong effect on the emittance dilution and energy distribution of

the bunch, and it is dominated by the radius of the disk aperture “a” [9], and a large “a” can suppress the SRW in two directions. In Fig. 3, “2a” is increased from 10 mm to 15 mm, and the longitudinal and transversal SRW can be suppressed by factors of 2 and 6, respectively.

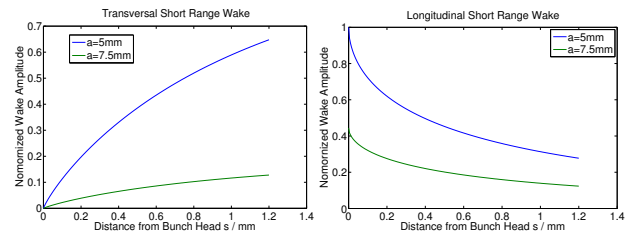


Figure 3: SRW distribution of different aperture radius.

Large “a” means high group velocity  $V_g$ . A high  $V_g$  can induce breakdown events easily and lower RF power efficiency. However, using a higher phase advance per cell can effectively lower the group velocity and maintain good RF efficiency [10].

Table 1 show the comparison between different modes of phase advance, which is calculated using SUPERFISH 7.0 [11]. The length of the structure, operation frequency, disk aperture radius “a” and disk width “t” for all types are fixed on 1 m, 5712 MHz, 7.5 mm and 2.5 mm respectively. In Table 1, the group velocity is decreased and the RF efficiency is improved, as the phase advance is changed from  $2\pi/3$  to  $5\pi/6$ . In these four modes,  $5\pi/6$  has the optimum group velocity and RF efficiency, but its phase stability is the poorest. So  $4\pi/5$  is the best compromise option with suitable group velocity, shunt impedance and phase stability.

Table 1: Comparison between Different Modes

( $L=1$  m,  $f_0=5712$  MHz,  $a=7.5$  mm,  $t=2.5$  mm)

Operating mode	Group velocity $V_g/c$ (%)	Shunt impedance $R$ ( $M\Omega/m$ )	Phase stability $d\theta/df$ ( $^\circ/MHz$ )	Attenuation factor $\tau$
$2\pi/3$	3.441	64.50	0.61	0.1748
$3\pi/4$	2.846	63.43	0.84	0.1954
$4\pi/5$	2.356	69.96	1.07	0.2267
$5\pi/6$	1.986	69.31	1.32	0.2622

In Table 1, an attenuation factor 0.2267 of  $4\pi/5$  is lower than the optimum range, and the RF power is not effectively used, thus the structure length needs to be increased. Based on the overall considerations, 83 cells with 1.742 m are a better option, and the attenuation is improved to 0.4 which is better for power efficiency.

### Iris Optimization for Suppressing the RF Breakdown

In Section above, the last results for  $4\pi/5$  were not optimum, and the group velocity, peak field amplitude and RF efficiency may not satisfy the design target, thus further optimization of these factors is needed.

Surface electrical field and group velocity are two crucial factors of RF breakdown [10], and suppressing them can realize better performance of the RF breakdown.

Both the peak field and group velocity are influenced by the iris shape. According to the simulations, a proper elliptical disk iris and disk width can suppress the peak electrical field, thus the two axes of elliptic iris tip in Fig. 4 should be tuned for the optimal peak electrical field and group velocity.

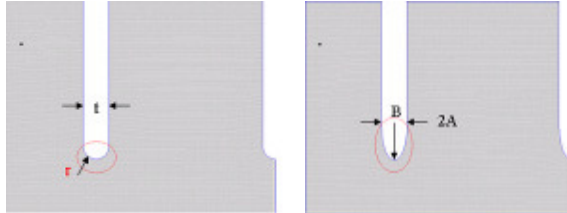


Figure 4: Two types of iris shape of disk-loaded cell.

Before tuning the iris, the disk aperture radius “a” is fixed at 7.5 mm for the specific wakefield, and the two axes of the ellipse curve, in which the transversal radius 2A is equal to t, are varied over the specific range for peak field and group velocity analysis. The ranges of 2A and 2B are varied from 2.5 cm to 4.5 cm to reveal some underlying potential for optimization.

In Fig. 5-A, clearly the peak electrical field is suppressed by lengthening both axes 2A and 2B, and there is a trough for most curves. In Fig. 5-B, the suppression of the group velocity is dominated by lengthening 2A, which also rises slightly as 2B increases.

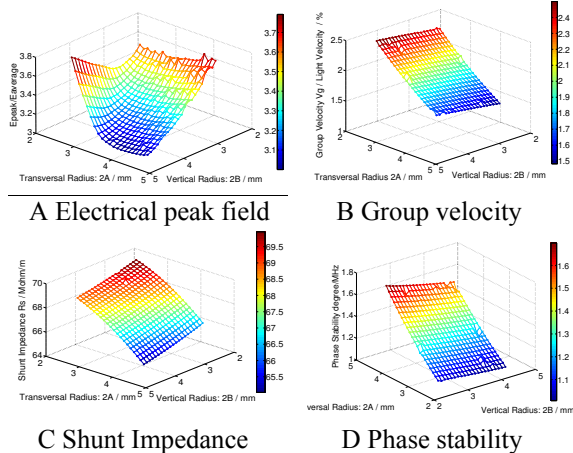


Figure 5: Different parameters as 2A and 2B.

According to the results in Figs. 5-A, B, it is easy to reach the design target for the desired peak field and group velocity by tuning both axes of the elliptic iris, especially 2A. However the shunt impedance in Fig. 5-C and the phase stability in Fig. 5-D are also dominated by 2A. In Fig. 5-C, the smaller shunt impedance for larger values of 2A and 2B results in more power dissipation by disk-loaded cells. In Fig. 5-D, the stability of the phase advance per cell deteriorates as 2A increases, and improves slightly as 2B increases.

According to the analysis above, 2A is clearly the crucial factor for optimizing, and 2B is the assistant parameter for slightly optimization. Based on this results, a optimum point of 2A=5mm and 2B=9mm is found. At this point, the ratio of the peak electrical field to average field is about 2.6, and the group velocity is about 1.7 % of light velocity, the impedance is about 62 Mohm/m and the phase stability is about 1.5°/MHz, as shown in Fig. 6.

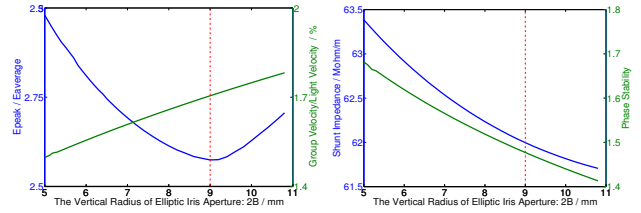


Figure 6: Parameters at optimum point.

Summarizing the results in Sections 2 and 3, an optimization scheme is proposed for the C-band accelerating structure system, as summarized in Table 2.

Table 2: Parameters of the Optimized C-band Traveling-wave Accelerating Structure

C-band system	SLED-II + CG
Phase advance per cell	$4\pi/5$
Length of cell	20.994 mm
Length of total cells	1.784 m
Average 2a	15 mm
Elliptical tip radius: 2B/2A	9 mm/5 mm
Width of iris: t	5 mm
Peak electric field: $E_{peak}/E_0$	2.6
Shunt impedance: $R_s$	Ave: 62 Mohm/m
Q factor	Ave: 10470
Group velocity : $vg/c$	Ave: 1.7 %
Filling time	340 ns
Attenuation factor: $\tau$	0.585

### CONCLUSION

C-band high gradient accelerating structure is a key technique of the linac for a compact XFEL facility at SINAP, and now the first prototype of high power model is read and the relative design optimization offers a remarkable improvement in the performance of a C-band accelerating structure for the development of robust C-band accelerating structure.

### ACKNOWLEDGEMENT

It's grateful to Dr. Juwen Wang of SLAC for his helpful suggestions and useful discussion.

### REFERENCES

[1] C. Feng et al, Chinese Sci Bull, 2010, Vol.55 No.3: 221-227  
 [2] M. Jiang et al, Chinese Sci Bull, 2009, Vol.54 No.22: 4171-4181

- [3] W. Fang et al, Chinese Sci Bull, 2011, Vol.56 No.1: 18-23
- [4] T. Inagaki et al, PAC07, 2007, 2766-2768
- [5] T. Sakura et al, PAC09, 2009, 1563-1565
- [6] Charles W. Steele, 1966, VOL. MTT-14, NO. 2
- [7] T. Khabiboulline et al, 1995, DESY M-95-02
- [8] W. Fang et al, accepted by Chinese Sci Bull
- [9] K. Bane et al, 1997, DESY M-97-02
- [10] Z. Li et al, SLAC-PUB-11916
- [11] J. Billen et al, LA-UR-96-1834
- [12] T. Shintake et al, LINAC2002, 43-45